applied sciences

MDPI

Article

Influence of Induced Magnetic Field on Free Convection of Nanofluid Considering Koo-Kleinstreuer-Li (KKL) Correlation

M. Sheikholeslami [1], Q. M. Zaigham Zia [2] and R. Ellahi [3,4,*]

[1] Department of Mechanical Engineering, Babol University of Technology, Babol 484, Iran; mohsen.sheikholeslami@yahoo.com
[2] Department of Mathematics, COMSATS Institute of Information Technology, Park Road, Chak Shahzad, Islamabad 45550, Pakistan; zaighum_zia@comsats.edu.pk
[3] Department of Mathematics & Statistics, FBAS, IIUI, H-10 Sector, Islamabad 44000, Pakistan
[4] Mathematics Faculty of Science Taibah University, Madinah 41411, Munawwarah, Saudi Arabia
* Correspondence: rellahi@engr.ucr.edu or rahmatellahi@yahoo.com

Academic Editor: Fan-Gang Tseng
Received: 3 September 2016; Accepted: 24 October 2016; Published: 2 November 2016

Abstract: In this paper, the influence of induced magnetic field on free convection of Al_2O_3-water nanofluid on permeable plate by means of Koo-Kleinstreuer-Li (KKL) model is reported. Impact of Brownian motion, along with the properties of nanofluid, are also taken into account. The resulting equations are solved utilizing Runge-Kutta integration method. Obtained results are examined for innumerable energetic parameters, namely Al_2O_3 volume fraction, suction parameter, and Hartmann and magnetic Prandtl numbers. Results indicate that the velocity profile reduces with rise of the suction parameter and magnetic Prandtl and Hartmann numbers but it increases with addition of nanoparticles. Shear stress enhances with rise of suction parameter, magnetic Prandtl and Hartmann numbers. Temperature gradient improves with augment of suction parameter.

Keywords: induced magnetic field; nanofluid; free convection; permeable plate; current density

1. Introduction

Magnetohydrodynamic (MHD) free convection has several applications, such as combustion modeling, geophysics, fire engineering, etc. In recent decades, nanotechnology has been presented as a new passive technique for heat transfer improvement. MHD nanofluid natural convection in a tilted wavy cavity has been presented by Sheremet et al. [1]. They illustrated that a change of titled angle causes convective heat transfer to be enhanced. 3D MHD free convective heat transfer was examined by Sheikholeslami and Ellahi [2] using Lattice Boltzmann method (LBM). Their results showed that Lorentz forces cause the temperature gradient to reduce. Ismael et al. [3] investigated the influence of Lorentz forces on nanofluid flow in an enclosure with moving walls. Their outputs indicated that the impact of Lorentz forces reduces with direction of magnetic field. Sheikholeslami and Ellahi [4] utilized LBM to study Fe_3O_4-water flow, with the aim of drug delivery. They concluded that the velocity gradient reduces with the rise of magnetic number. The influence of non-uniform Lorentz forces on nanofluid flow style has been studied by Sheikholeslami Kandelousi [5]. He concluded that improvement in heat transfer reduces with rise of Kelvin forces. A new model for nanofluid on peristaltic flow was presented by Tripathi and Beg [6]. They reported different behavior for nanofluid temperature profiles with changing temperature. Kouloulias et al. [7] presented an experimental analysis for free convection of nanofluid. They showed that greater nanoparticle volume fraction leads to higher Rayleigh numbers.

The influence of thermal radiation on magnetohydrodynamic nanofluid motion has been reported by Sheikholeslami et al. [8]. They concluded that the nanofluid concentration gradient augments with the rise of the radiation parameter. Mineral oil-based nanofluids have been utilized in natural convection by Peña et al. [9]. MHD Fe_3O_4-water flow in a wavy cavity with moving wall has been investigated by Sheikholeslami and Chamkha [10]. The influence of Lorentz forces on forced convective heat transfer has been examined by Sheikholeslami et al. [11]. They illustrated that a greater Reynolds number has a more sensible effect on Kelvin forces. Akbar and Khan [12] investigated the impact of magnetic field on nanofluid motion in an asymmetric channel. Hakeem et al. [13] studied the influence of Lorentz forces on various nanofluids by means of second order slip flow mode. They showed that a unique solution exists for this problem for high Hartman number values. Several researchers have investigated about this subject [14–22].

In almost all the previous papers, the authors neglected the induced magnetic field. However, in various physical states it is necessary to consider this effect in governing equations. This assumption is considered in order to simplify the mathematical analysis of the problem. Furthermore, the induced magnetic field produces its own magnetic field in the fluid; therefore, it can amend the original magnetic field. Also, nanofluid motion in the magnetic field produces mechanical forces which change the motion of motion. Ghosh et al. [23] reported the impact of induced Lorentz forces on temperature profile. Unsteady magnetohydrodynamic flow on a cone has been investigated by Vanita and Kumar [24]. Beg et al. [25] examined the impact of induced magnetic field on boundary layer flow. The influence of atherosclerosis on hemodynamics of stenosis has been forecasted by Nadeem and Ijaz [26]. They showed that the velocity gradient on the wall of titled arteries reduces with augment of Strommers number.

The chief end of this paper is to illustrate the influence of induced magnetic field on nanofluid hydrothermal treatment between two vertical plates. To obtain outputs, Runge-Kutta method is selected. The impacts of the suction parameter, magnetic Prandtl and Hartmann numbers, volume fraction of nanofluid on temperature, and induced magnetic, velocity and current density profiles are examined.

2. Problem Statement

Al_2O_3-water fluid through two vertical permeable sheets is investigated as illustrated in Figure 1. The boundary conditions are clear in this figure. The variables are only the function of y because plates are infinite. Velocity and magnetic field vectors are considered as $\vec{v} = [u, v_0, 0]$ and $\vec{b} = [b_x, b_0, 0]$ respectively. The governing equations and boundary conditions can be obtained as follows:

$$\upsilon_{nf}\frac{d^2u}{dy^2} + \frac{\mu_e b_0}{\rho_{nf}}\frac{db_x}{dy} + g\beta_{nf}\left(T - T_0\right) + v_0\frac{du}{dy} = 0 \tag{1}$$

$$\frac{1}{\mu_e\sigma_{nf}}\frac{d^2b_x}{dy^2} + b_0\frac{du}{dy} + v_0\frac{db_x}{dy} = 0 \tag{2}$$

$$\frac{k_{nf}}{\left(\rho C_p\right)_{nf}}\frac{d^2T}{dy^2} + v_0\frac{dT}{dy} = 0 \tag{3}$$

$$b_x\left(0\right) = 0, u\left(0\right) = 0, \frac{dT}{dy}\left(0\right) = -\frac{q}{k_f} \tag{4}$$

$$\frac{db_x}{dy}\left(h\right) = 0, u\left(h\right) = 0, T\left(h\right) = T_0 \tag{5}$$

$(\sigma)_{nf}$, $(\rho C_p)_{nf}$, $(\rho\beta)_{nf}$ and $\left(\rho_{nf}\right)$ can be introduced as [3]:

$$\begin{array}{ll} \frac{\sigma_{nf}}{\sigma_f} = 1 + \frac{3(\sigma_p/\sigma_f - 1)\phi}{(\sigma_p/\sigma_f + 2) - (\sigma_p/\sigma_f - 1)\phi}, & (\rho\beta)_{nf} = (1-\phi)(\rho\beta)_f + (\rho\beta)_p\,\phi, \\ (\rho\, C_p)_{nf} = \phi(\rho\, C_p)_p + (\rho\, C_p)_f(1-\phi), & \rho_{nf} = \phi\rho_p + \rho_f(1-\phi) \end{array} \tag{6}$$

$\left(k_{nf}\right)$ and $\left(\mu_{nf}\right)$ are obtained according to Koo-Kleinstreuer-Li (KKL) model [27]:

$$\begin{array}{l} k_{nf} = \frac{3(k_p/k_f - 1)\phi}{-(k_p/k_f - 1)\phi + (k_p/k_f + 2)} + 1 + 5\phi \times 10^4 c_{p,f}\, g'(d_p, T, \phi)\rho_f \sqrt{\frac{\kappa_b T}{\rho_p d_p}} \\ g'\left(d_p, T, \phi\right) = \\ \left(a_1 + a_2 Ln\left(d_p\right) + a_5 Ln\left(d_p\right)^2 + a_3 Ln\left(\phi\right) + a_4 \ln\left(d_p\right) Ln\left(\phi\right)\right) Ln\left(T\right) + \\ \left(a_6 + a_7 Ln\left(d_p\right) + a_{10} Ln\left(d_p\right)^2 + a_8 Ln\left(\phi\right) + a_9 \ln\left(d_p\right) Ln\left(\phi\right)\right) \\ R_f = d_p\left(1/k_{p,eff} - 1/k_p\right), R_f = 4 \times 10^{-8} km^2/W \end{array} \tag{7}$$

$$\mu_{nf} = \frac{\mu_f}{(1-\phi)^{2.5}} + \frac{k_{Brownian}}{k_f} \times \frac{\mu_f}{\Pr} \tag{8}$$

All needed coefficients and properties are illustrated in Tables 1 and 2 [27].
Dimensionless parameters are presented as:

$$\begin{array}{l} U = \frac{\upsilon u}{g\beta h^2 \Delta T}, B = \sqrt{\frac{\mu_e}{\rho_f}}\upsilon_f b_x \left(g\beta_f h^2 \Delta T\right)^{-1}, \theta = \Delta T^{-1}\left(T - T_0\right), \Delta T = qh/k_f, Y = \frac{y}{h} \\ \Pr = \left(\rho C_p\right)_f \frac{\mu_f}{k_f}, Pm = \mu_e \upsilon_f \sigma_f, Ha = \frac{B_0 h}{\upsilon_f}\sqrt{\frac{\mu_e}{\rho}}, V_0 = \frac{v_0 h}{\upsilon_f} \end{array} \tag{9}$$

Finally, the dimensionless governing equations are

$$\frac{d^2U}{dY^2} + \frac{Ha}{A_2}\frac{dB}{dY} + \frac{A_1 A_6}{A_2}\theta + \frac{A_1}{A_2}V_0\frac{dU}{dY} = 0 \tag{10}$$

$$\frac{d^2B}{dY^2} + A_5 V_0 Pm\frac{dB}{dY} + A_5 Ha Pm\frac{dU}{dY} = 0 \tag{11}$$

$$\frac{d^2\theta}{dY^2} + \frac{A_3}{A_4}V_0 \Pr\frac{d\theta}{dY} = 0 \tag{12}$$

$$B\left(0\right) = 0, U\left(0\right) = 0, \frac{d\theta}{dY}\left(0\right) = -1 \tag{13}$$

$$\frac{dB}{dY}\left(1\right) = 0, U\left(1\right) = 0, \theta\left(1\right) = 0 \tag{14}$$

Induced current density can be defined:

$$J = -dB/dY \tag{15}$$

C_f and Nu can be expressed as:

$$C_f = \frac{A_2}{A_1}U'(0), Nu = A_4/\theta(0). \tag{16}$$

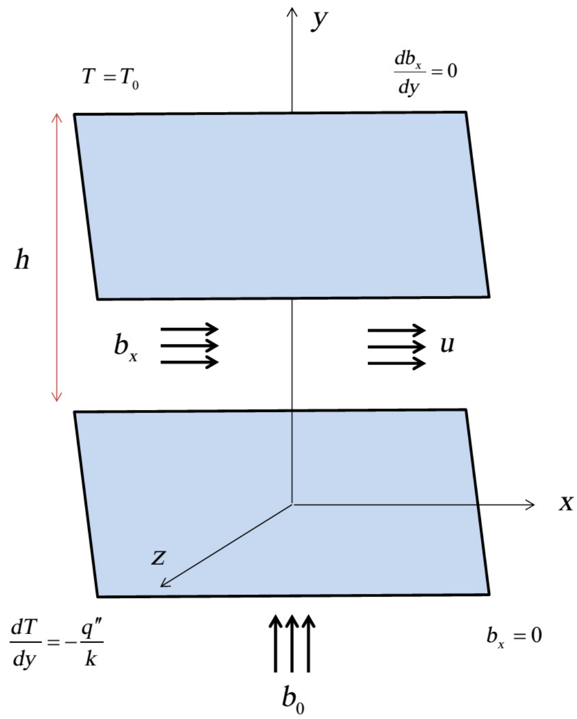

Figure 1. Geometry of the problem.

Table 1. Constants of Al_2O_3 − Water [27].

Coefficient Values	Al_2O_3 − Water
a_1	52.813
a_2	6.115
a_3	0.695
a_4	4.1×10^{-2}
a_5	0.176
a_6	−298.198
a_7	−34.532
a_8	−3.922
a_9	−0.235
a_{10}	−0.999

Table 2. Properties of water and Al_2O_3 [27].

Material	ρ (kg/m^3)	C_p (j/kg·k)	k (W/m·k)	$\beta \times 10^5$ (K^{-1})	d_p (nm)	σ (Ω·m)$^{-1}$
Pure water	997.1	4179	0.613	21	-	0.05
Al_2O_3	3970	765	25	0.85	47	1×10^{-10}

3. Runge-Kutta Method

In Runge-Kutta method, at first the following definitions are applied: $x_2 = U, x_1 = Y, x_3 = U'$, $x_4 = B, x_5 = B', x_6 = \theta, x_7 = \theta'$. The final system and initial conditions are:

$$\begin{pmatrix} {x_1}' \\ {x_2}' \\ {x_3}' \\ {x_4}' \\ {x_5}' \\ {x_6}' \\ {x_7}' \end{pmatrix} = \begin{pmatrix} 1 \\ x_3 \\ \frac{1}{A_2}\left[-Hax_5 - A_1 A_6 x_6 - A_1 V_0 x_3\right] \\ x_5 \\ -A_5 V_0 x_5 Pm - A_5 x_3 HaPm \\ x_7 \\ -\frac{A_3}{A_4} V_0 x_7 \mathrm{Pr} \end{pmatrix} \tag{17}$$

$$\begin{pmatrix} 0 \\ 0 \\ u_1 \\ 0 \\ u_2 \\ u_3 \\ -1 \end{pmatrix} = \begin{pmatrix} x_1 \\ x_2 \\ x_3 \\ x_4 \\ x_5 \\ x_6 \\ x_7 \end{pmatrix} \tag{18}$$

Equations (17) and (18) are solved utilizing fourth order Runge-Kutta method. According to $U(1) = 0, B'(1) = 0, \theta(1) = 0$, unknown initial conditions can be obtained by Newton's method.

4. Results and Discussion

Steady two-dimensional nanofluid hydrothermal treatment between two parallel vertical permeable plates is studied considering induced magnetic field. The Runge-Kutta integration scheme is utilized to solve this problem. MAPLE code has been validated by comparison with a previously published paper [28]. Table 3 indicates good accuracy of present code. The influences of important parameters such as magnetic Prandtl number (Pm), Hartmann number (Ha), suction parameter (V_0) and nanoparticle volume fraction (ϕ) on flow style are examined.

Table 3. Comparison of skin friction tension over the upper wall between the present results and previous work. H_a, Hartmann number; V_0, suction parameter; Pr, Prandtl number.

V_0	Pr	Pr_m	Ha	Sarveshanand and Singh [21]	Present Work
0.5	0.7	0.5	5	0.016	0.015
0.75	0.7	0.5	5	0.011	0.011
1	0.7	1	5	0.018	0.018
1	0.015	0.5	0.5	2.695	2.700

Impact of ϕ on induced magnetic field, current density, temperature and velocity distributions is shown in Figure 2. As volume fraction of nanofluid augments, nanofluid velocity and temperature are enhanced due to an increase in fluid motion by adding nanoparticles. Induced current density increases with an augment of ϕ while the opposite behavior is shown for induced magnetic field. Influence of suction parameter on hydrothermal behavior is depicted in Figure 3. Velocity, temperature and induced current density decreases, with an augment of suction parameter while induced magnetic field enhances with rise of V_0. Therefore, this parameter can be considered as control parameter for engineering designs.

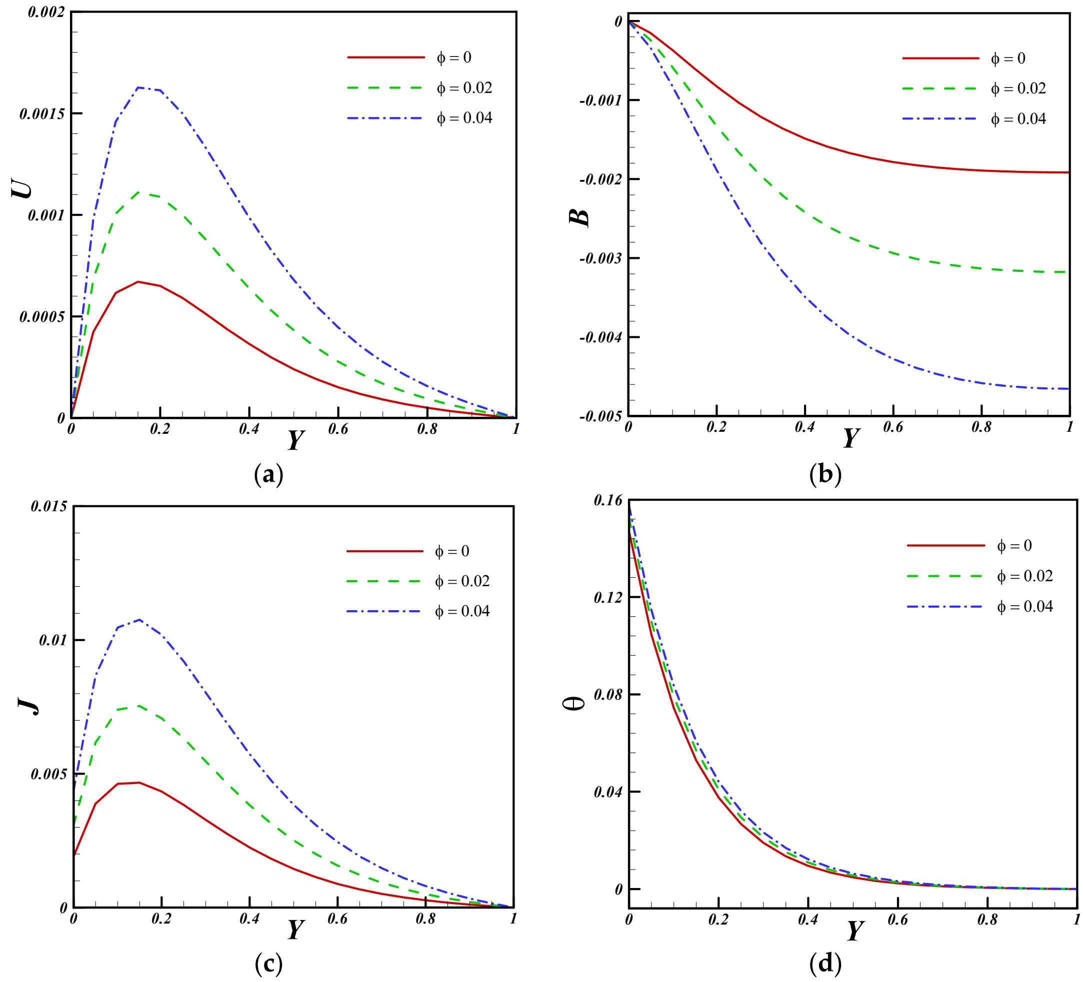

Figure 2. Effect of nanoparticle volume fraction on velocity (**U**); induced magnetic field (**B**); induced current density (**J**) and temperature field (**θ**) distributions when $V_0 = 1,\ Ha = 5,\ Pm = 1,\ \Pr = 6.8$. Magnetic Prandtl number: Pm; nanoparticle volume fraction: ϕ.

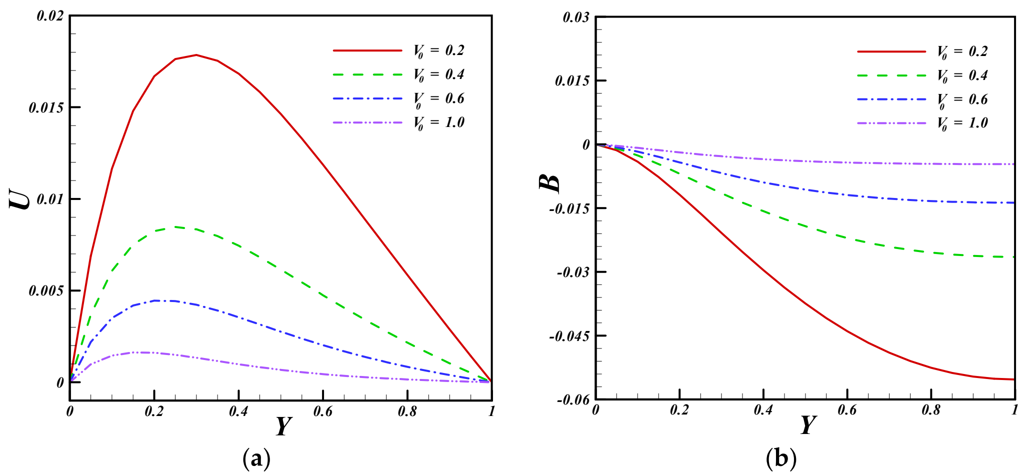

Figure 3. *Cont.*

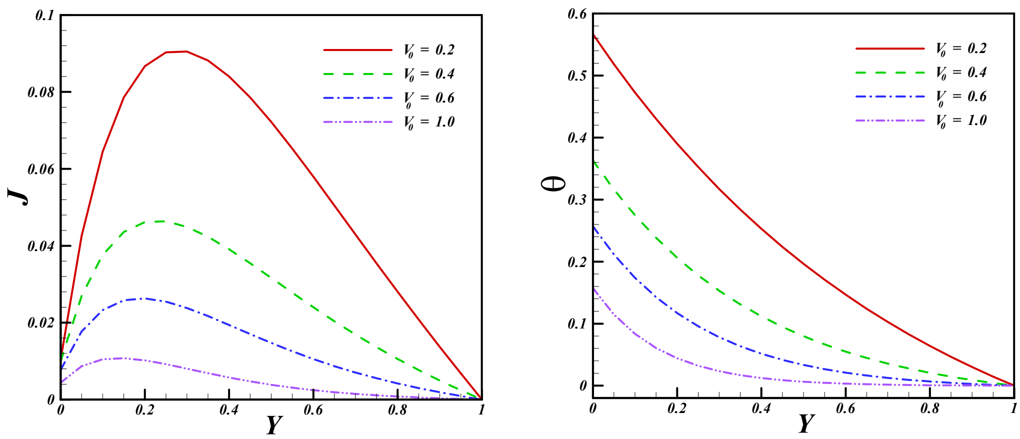

(**c**) (**d**)

Figure 3. Effect of suction parameter on velocity (**U**); induced magnetic field (**B**); induced current density (**J**) and induced temperature field (θ) distributions when $Ha = 5,\ Pm = 1,\ \phi = 0.04,\ \Pr = 6.8$.

Figure 4 depicts the impacts of Lorentz forces on induced magnetic field, induced current density and velocity distributions. As Lorentz forces augments, the back flow appears and in turn velocity of nanofluid decreases. In addition, it can be seen that the maximum velocity point shifts to the hot wall. Induced magnetic field decreases with rise of magnetic field strength but induced current density is enhanced with the rise of Lorentz forces. Influence of Pm on induced magnetic field, induced current density and velocity profiles is depicted in Figure 5. Without the magnetic field, the shape of the velocity profiles is parabolic but in the existence of the magnetic field its shape changes to being flattened. The nanofluid motion and induced magnetic field reduces with an augment of Pm. Induced current density rises with augment of Pm.

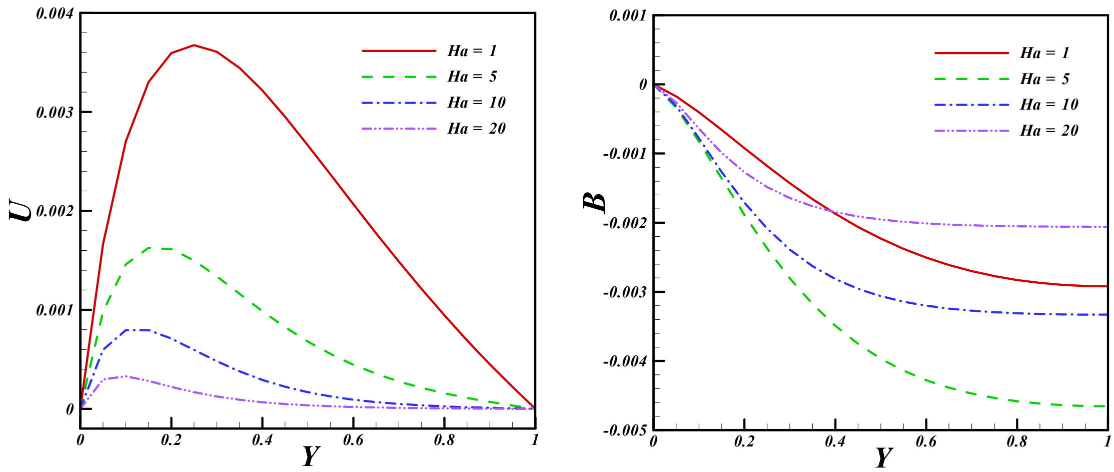

(**a**) (**b**)

Figure 4. *Cont.*

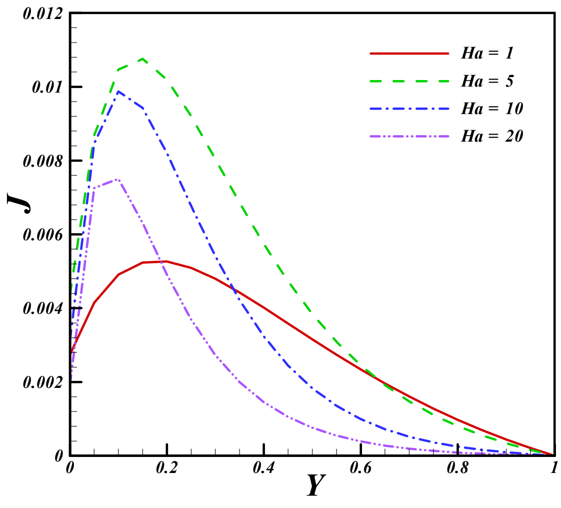

(**c**)

Figure 4. Effect of Hartmann number (Ha) on velocity (**U**); induced magnetic field (**B**) and induced current density (**J**) distributions when $V_0 = 1$, $Pm = 1$, $\phi = 0.04$, $\mathrm{Pr} = 6.8$.

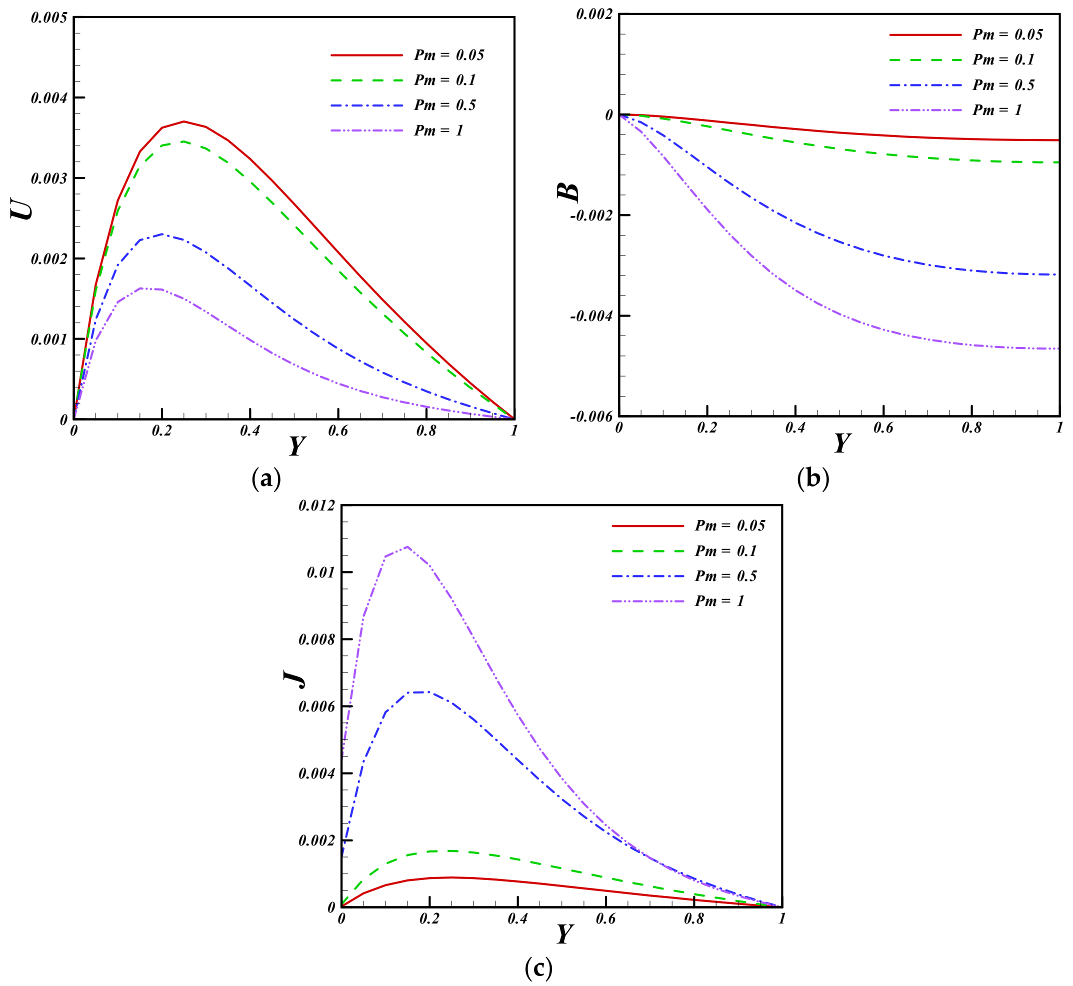

Figure 5. Effect of magnetic Prandtl number (Pm) on velocity (**U**); induced magnetic field (**B**) and induced current density (**J**) distributions when $V_0 = 1$, $Ha = 5$, $\phi = 0.04$, $\mathrm{Pr} = 6.8$.

Influences of magnetic Prandtl number (Pm), Hartmann number (Ha), suction parameter (V_0) and nanoparticle volume fraction (ϕ) on skin friction coefficient are depicted in Figures 6 and 7. According to these data, a correlation is presented for skin friction coefficient as follows:

$$\begin{aligned} C_f &= 0.25335 - 0.34173V_0 - 0.011146Ha - 0.12279\phi \\ &+0.0076966V_0\ Ha + 0.079691V_0\ Pm - 2.54355V_0\ \phi \\ &+0.00154943Ha\ Pm - 0.0424Ha\ \phi - 1.15754Pm\ \phi \\ &+0.11737V_0^2 + 0.0001179Ha^2 + 0.033354Pm^2 + 13.69282\phi^2 \end{aligned} \tag{19}$$

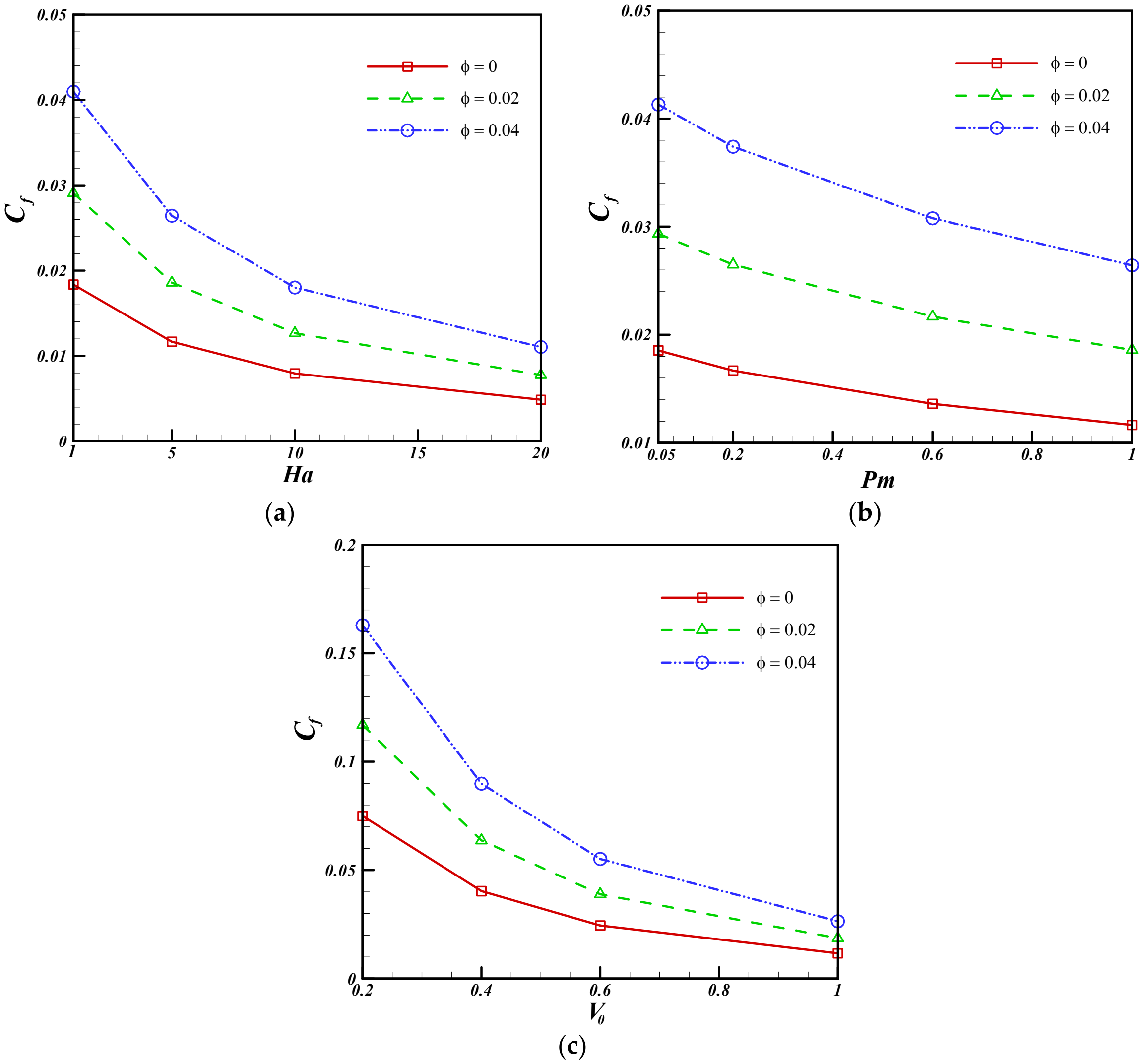

Figure 6. Influences of magnetic Prandtl number (Pm), Hartmann number (Ha), suction parameter (V_0) and nanoparticle volume fraction (ϕ) on skin friction coefficient $\left(C_f\right)$ when Pr $=$ 6.8. (**a**) $V_0 = 1,\ Pm = 1$; (**b**) $V_0 = 1,\ Ha = 5$; (**c**) $Ha = 5,\ Pm = 1$.

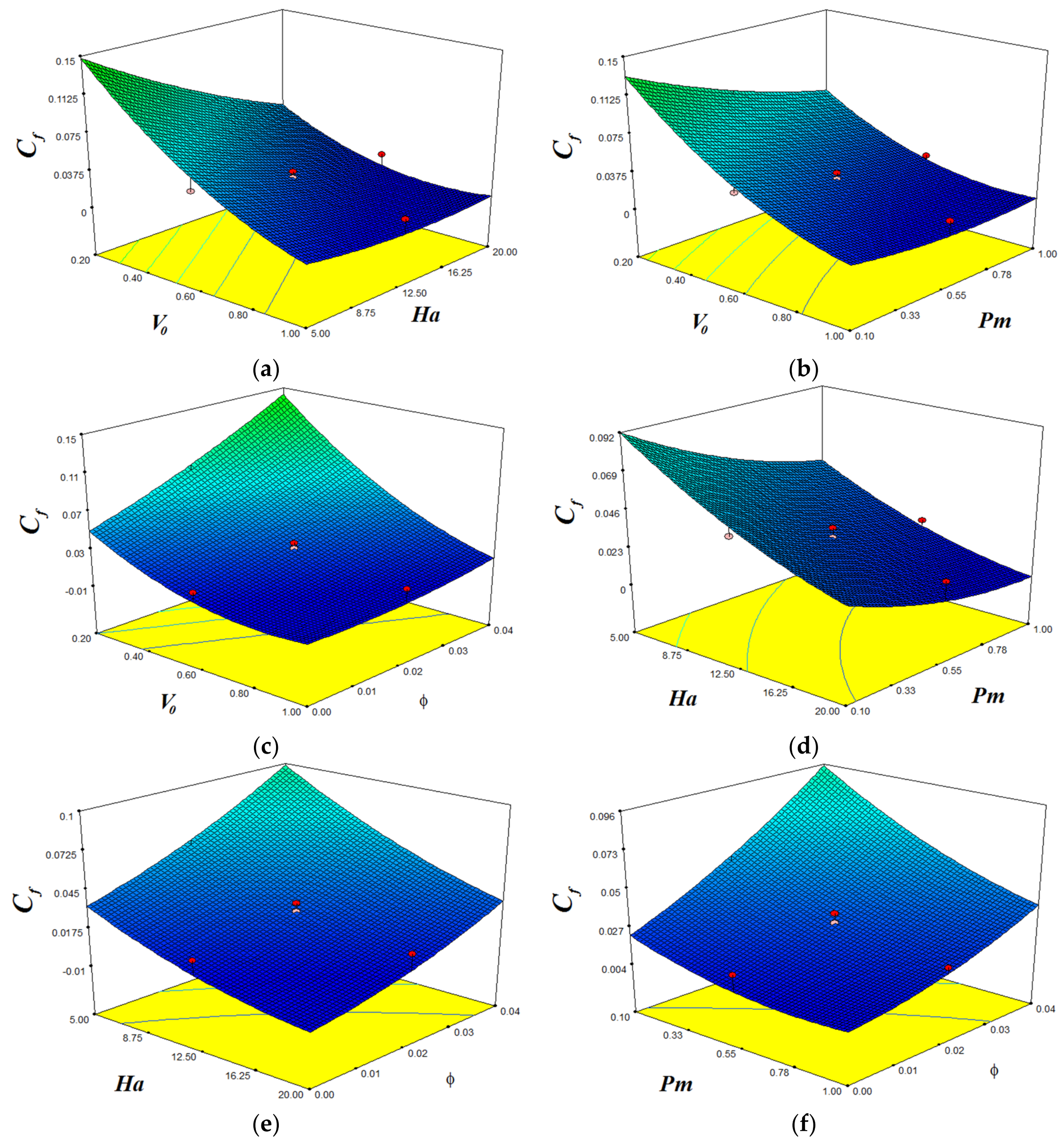

Figure 7. 3D surface plots for skin friction coefficient. (**a**) $Pm = 0.55,\ \phi = 0.02$; (**b**) $Ha = 12.5,\ \phi = 0.02$; (**c**) $Ha = 12.5,\ Pm = 0.55$; (**d**) $V_0 = 0.6,\ \phi = 0.02$; (**e**) $V_0 = 0.6,\ Pm = 0.55$; (**f**) $V_0 = 0.6$, Ha = 12.5.

It can be concluded that C_f has reverse relationship with all active parameters except for ϕ. Figure 8 shows the influence of V_0 and ϕ on Nusselt number. In addition, a good correlation has been presented for the Nusselt number as follows:

$$\begin{array}{l} Nu = 0.80342 + 4.92333V_0 + 1.72177\phi - 3.50195V_0\phi \\ +1.822V_0^2 - 0.75963\phi^2 \end{array} \tag{20}$$

As suction parameter (V_0) and nanoparticle volume fraction (ϕ) increase, temperature gradient increases. Therefore, Nu is enhanced with enhancement of V_0, ϕ.

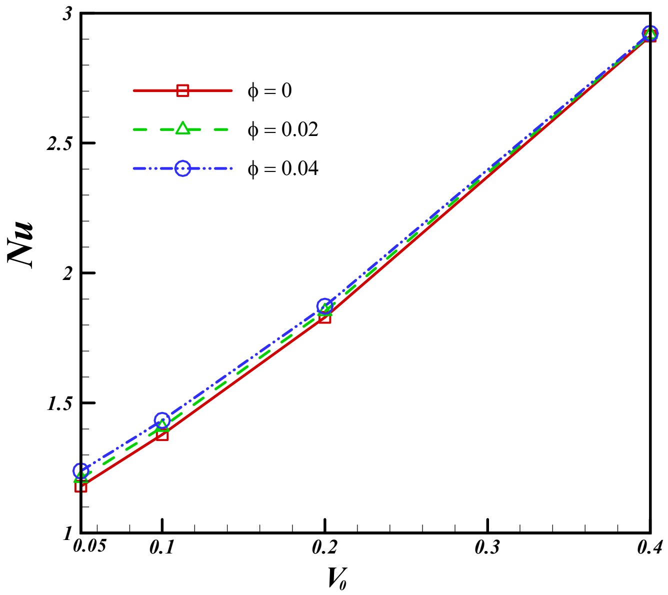

(**a**)

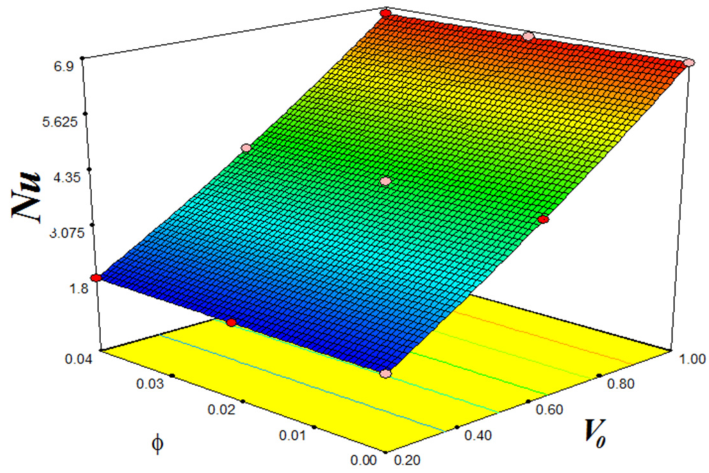

(**b**)

Figure 8. Influence of nanofluid volume fraction (ϕ) and suction parameter (V_0) on Nusselt number (Nu) when $Ha = 5,\ Pm = 1,\ \Pr = 6.8$.

5. Conclusions

The influence of induced magnetic field on nanofluid motion and forced convection between two vertical permeable plates is investigated. To solve coupled equations, Runge-Kutta method is utilized. The influence of different dimensionless parameters on induced magnetic field, velocity and temperature distributions are considered. Results illustrate that current density augments with a rise of volume fraction of nanofluid and Hartmann and magnetic Prandtl numbers, while it is reduced with a rise in the suction parameter. As Lorentz force increases, velocity and induced magnetic field are reduced and maximum velocity point shifts to the left side.

Acknowledgments: R. Ellahi is grateful to Sultan Z Alamri, Dean Faculty of Science and Yousef Alharbi, Chairman Mathematics Department, Taibah University, Madinah Munawwarah, Saudi Arabia for their kind cooperation. R. Ellahi is also thankful to PCST to honed him with 7th top most Productive Scientist Award in category A and Thomson Reuters to rank him among top 1% highly cited researchers on Web of Science in 2015–2016.

Author Contributions: This paper is contributed in all respect by M. Sheikholeslami, Q. M. Zaigham Zia and R. Ellahi equally.

Conflicts of Interest: The authors declare no conflict of interest.

Nomenclature

B	Dimensionless induced horizontal magnetic field
$\vec{v}$	Velocity vector
$\vec{b}$	Vector of magnetic field
k	Thermal conductivity
c_p	Specific heat
J	Induced current density
T	Temperature
Ha	Hartmann number
Pr	Prandtl number
V_0	Suction parameter
Pm	Magnetic Prandtl number
U	Dimensionless horizontal velocity

Greek Symbols

η	Dimensionless distance
β	Coefficient of thermal expansion
σ	Electrical conductivity
μ	Dynamic viscosity of nanofluid
θ	Dimensionless temperature
ϕ	Nanofluid volume fraction
ρ	Density

Subscripts

p	Solid
f	Base fluid

References

1. Sheremet, M.A.; Oztop, H.F.; Pop, I. MHD natural convection in an inclined wavy cavity with corner heater filled with a nanofluid. *J. Magn. Magn. Mater.* **2016**, *416*, 37–47. [CrossRef]
2. Sheikholeslami, M.; Ellahi, R. Three dimensional mesoscopic simulation of magnetic field effect on natural convection of nanofluid. *Int. J. Heat Mass Transf.* **2015**, *89*, 799–808. [CrossRef]
3. Ismael, M.A.; Mansour, M.A.; Chamkha, A.J.; Rashad, A.M. Mixed convection in a nanofluid filled-cavity with partial slip subjected to constant heat flux and inclined magnetic field. *J. Magn. Magn. Mater.* **2016**, *416*, 25–36. [CrossRef]
4. Sheikholeslami, M.; Ellahi, R. Simulation of ferrofluid flow for magnetic drug targeting using Lattice Boltzmann method. *J. Z. Naturforschung A* **2015**, *70*, 115–124.
5. Kandelousi, M.S. Effect of spatially variable magnetic field on ferrofluid flow and heat transfer considering constant heat flux boundary condition. *Eur. Phys. J. Plus* **2014**, *129*, 248. [CrossRef]
6. Tripathi, D.; Beg, O.A. A study on peristaltic flow of nanofluids: Application in drug delivery systems. *Int. J. Heat Mass Transf.* **2014**, *70*, 61–70. [CrossRef]
7. Kouloulias, K.; Sergis, A.; Hardalupas, Y. Sedimentation in nanofluids during a natural convection experiment. *Int. J. Heat Mass Transf.* **2016**, *101*, 1193–1203. [CrossRef]
8. Sheikholeslami, M.; Ganji, D.D.; Younus Javed, M.; Ellahi, R. Effect of thermal radiation on magnetohydrodynamics nanofluid flow and heat transfer by means of two phase model. *J. Magn. Magn. Mater.* **2015**, *374*, 36–43. [CrossRef]

9. Cadena-de la Peña, N.L.; Rivera-Solorio, C.I.; Payán-Rodríguez, L.A.; García-Cuéllar, A.J.; López-Salinas, J.L. Experimental analysis of natural convection in vertical annuli filled with AlN and TiO_2/mineral oil-based nanofluids. *Int. J. Therm. Sci.* **2017**, *111*, 138–145. [CrossRef]
10. Sheikholeslami, M.; Chamkha, A.J. Flow and convective heat transfer of a ferro-nanofluid in a double-sided lid-driven cavity with a wavy wall in the presence of a variable magnetic field. *Numer. Heat Transf. Part A* **2016**, *69*, 1186–1200. [CrossRef]
11. Sheikholeslami, M.; Vajravelu, K.; Rashidi, M.M. Forced convection heat transfer in a semi annulus under the influence of a variable magnetic field. *Int. J. Heat Mass Transf.* **2016**, *92*, 339–348. [CrossRef]
12. Akbar, N.S.; Khan, Z.H. Influence of magnetic field for metachoronical beating of cilia for nanofluid with Newtonian heating. *J. Magn. Magn. Mater.* **2015**, *381*, 235–242. [CrossRef]
13. Hakeem, A.K.A.; Ganesh, N.V.; Ganga, B. Magnetic field effect on second order slip flow of nanofluid over a stretching/shrinking sheet with thermal radiation effect. *J. Magn. Magn. Mater.* **2015**, *381*, 243–257. [CrossRef]
14. Sheikholeslami, M.; Ellahi, R.; Hassan, M.; Soleimani, S. A study of natural convection heat transfer in a nanofluid filled enclosure with elliptic inner cylinder. *Int. J. Numer. Methods Heat Fluid Flow* **2014**, *24*, 1906–1927. [CrossRef]
15. Sheikholeslami, M.; Ellahi, R. Electrohydrodynamic nanofluid hydrothermal treatment in an enclosure with sinusoidal upper wall. *Appl. Sci.* **2015**, *5*, 294–306. [CrossRef]
16. Mamourian, M.; Shirvan, K.M.; Ellahi, R.; Rahimi, A.B. Optimization of mixed convection heat transfer with entropy generation in a wavy surface square lid-driven cavity by means of Taguchi approach. *Int. J. Heat Mass Transf.* **2016**, *102*, 544–554. [CrossRef]
17. Ellahi, R.; Bhatti, M.M.; Riaz, A.; Sheikholeslami, M. Effects of magnetohydrodynamics on peristaltic flow of jeffrey fluid in a rectangular duct through a porous medium. *J. Porous Media* **2014**, *17*, 143–157. [CrossRef]
18. Ellahi, R.; Hassan, M.; Zeeshan, A. Aggregation effects on water base Al_2O_3 nanofluid over permeable wedge in mixed convection. *Asia-Pac. J. Chem. Eng.* **2016**, *11*, 179–186. [CrossRef]
19. Akbar, N.S. Ferromagnetic CNT suspended H_2O+Cu nanofluid analysis through composite stenosed arteries with permeable wall. *Phys. E Low-Dimens. Syst. Nanostruct.* **2015**, *72*, 70–76. [CrossRef]
20. Afsar Khan, A.; Ellahi, R.; Mudassar Gulzar, M.; Sheikholeslami, M. Effects of heat transfer on peristaltic motion of Oldroyd fluid in the presence of inclined magnetic field. *J. Magn. Magn. Mater.* **2014**, *372*, 97–106. [CrossRef]
21. Mahian, O.; Kianifar, A.; Kalogirou, S.A.; Pop, I.; Wongwises, S. A review of the applications of nanofluids in solar energy. *Int. J. Heat Mass Transf.* **2013**, *57*, 582–594. [CrossRef]
22. Ahmad, S.; Rohni, A.M.; Pop, I. Blasius and sakiadis problems in nanofluids. *Acta Mech.* **2011**, *218*, 195–204. [CrossRef]
23. Ghosh, S.K.; Beg, O.A.; Zueco, J. Hydromagnetic free convection flow with induced magnetic field effects. *Meccanica* **2010**, *14*, 175–185. [CrossRef]
24. Anand Kumar, V. Numerical study of effect of induced magnetic field on transient natural convection over a vertical cone. *Alex. Eng. J.* **2016**, *55*, 1211–1223.
25. Beg, O.A.; Bekier, A.Y.; Prasad, V.R.; Zueco, J.; Ghosh, S.K. Non-similar, laminar, steady, electrically-conducting forced convection liquid metal boundary layer flow with induced magnetic field effects. *Int. J. Therm. Sci.* **2009**, *48*, 1596–1606. [CrossRef]
26. Nadeem, S.; Ijaz, S. Impulsion of nanoparticles as a drug carrier for the theoretical investigation of stenosed arteries with induced magnetic effects. *J. Magn. Magn. Mater.* **2016**, *410*, 230–241. [CrossRef]
27. Kandelousi, M.S. KKL correlation for simulation of nanofluid flow and heat transfer in a permeable channel. *Phys. Lett. A* **2014**, *378*, 3331–3339. [CrossRef]
28. Sarveshanand; Singh, A.K. Magnetohydrodynamic free convection between vertical parallel porous plates in the presence of induced magnetic field. *Springer Plus* **2015**, *4*, 333.